An Evaluation of Finite-Difference and Finite-Integration Time-Domain Modelling Tools for Ground Penetrating Radar Antennas

Craig Warren[1], Lara Pajewski[2], Alessio Ventura[2], Antonios Giannopoulos[1],
[1]School of Engineering, The University of Edinburgh, The King's Buildings, Edinburgh, EH9 3JL, UK
Craig.Warren@ed.ac.uk, , A.Giannopoulos@ed.ac.uk
[2]Department of Engineering, Roma Tre University, via Vito Volterra 62, 00146, Rome, Italy
lara.pajewski@uniroma3.it, alessioventura@hotmail.com

***Abstract*—The development of accurate and realistic models of Ground Penetrating Radar (GPR) antennas is being driven by research into quantitative amplitude information from GPR, improved GPR antenna designs, and better-performing forward simulations that can feed into inversion algorithms. The Finite-Difference Time-Domain (FDTD) method and Finite-Integration technique (FIT) are popular numerical mehtods for simulating electromagnetic wave propagation. Time-Domain methods are particularly well-suited to modelling ultra-wideband GPR antennas as a broad range of frequencies can be modelled with a single simulation. We present comparisons using experimental and simulated data from a Geophysical Survey Systems 1.5 GHz antenna and a MALÅ Geoscience 1.2 GHz antenna. The antennas were investigated in free space and over a lossy dielectric environment with a target. For the simulations we used a commercial solver – Computer Simulation Technology Microwave Studio (CST) – and a free open-source FDTD solver – gprMax. For each test scenario, phase and amplitude information from the antenna responses were compared. Generally, we found very good agreement between the experimental data and the two simulations.**

***Index Terms*—antenna, simulation, Finite-Difference Time-Domain, Ground Penetrating Radar.**

I. Introduction

Simulations of Ground Penetrating Radar (GPR) that have included models of the actual antenna details have been mainly of antennas used in academia or for research purposes [1], [2], [3], [4], [5], [6], [7], [8], [9], [10]. There has been very limited published work of GPR simulations with models of commercial antennas [11], [12], [13]. In fact, many simulations have used a theoretical infinitesimal dipole source to represent a real GPR antenna where only far-field behaviour or travel-time information was of interest, or where computational resources were limited. However, computing power is increasing dramatically and becoming more accessible – multi-core CPUs and gigabytes of RAM are now standard features on desktop and laptop machines, and many businesses and universities now have their own High-Performance Computing (HPC) systems. These computational advances have particularly benefitted volume-based numerical techniques such as the Finite-Difference Time-Domain (FDTD) method, and allowed larger and more complex problems to be investigated. This, coupled with the desire to investigate quantitative information from GPR, means detailed three dimensional (3D) FDTD models of realistic GPR antennas need to be created and used.

In Section II we briefly present the two simulation tools that were evaluated. In Sections III and IV we describe the commercial GPR antennas that were modelled and present comparisons of measured responses with simulated responses from the two software (a response refers to a time history of electric field values at a spatial location). These comparisons are made with the antennas in free space, as well as with the antennas over emulsions which simulate dielectric environments with embedded targets.

II. Simulation software

We evaluated two simulation software tools: gprMax, which uses Yees algorithm [14] to solve Maxwells equations in 3D, and Computer Simulation Technology Microwave Studio (CST), which implements the Finite Integration Technique (FIT).

A. *gprMax*

gprMax is free, open-source software that simulates electromagnetic wave propagation for numerical modelling of GPR, and is available at http://www.gprmax.com. It was originally developed in 1996 [15] when numerical modelling using the FDTD method and, in general, the numerical modelling of GPR were in their infancy. Over the past 19 years gprMax has been one of the most widely used simulation tools in the GPR community. It has been successfully used for a diverse range of applications in academia and industry [16], [17], [18], [19], [20], [21], and has been cited more than 200 times since 2005 [22].

gprMax has recently been redeveloped in Python [23] with a series of improvements made to existing features as well as the addition of several new advanced modelling features including: an unsplit implementation of higher order perfectly matched layers (PMLs) using a recursive integration approach; diagonally anisotropic materials; dispersive media using multiple

Debye, Drude or Lorenz expressions; improved soil modelling using a semi-empirical formulation for dielectric properties and fractals for geometric characteristics; rough surface generation; and the ability to embed complex transducers and targets [24].

B. Computer Simulation Technology Microwave Studio

CST is a well-established commercial software tool available at http://www.cst.com. It features a suite of different solvers that use the FIT, Finite Element Method, Method of Moments, and Transmission-line matrix method. In this study we employed the transient solver, which is a general-purpose time-domain electromagnetic simulator implementing the FIT. The FIT is a spatial discretization scheme to numerically solve electromagnetic field problems and can yield results in both time and spectral domains. It was proposed in 1977 by Thomas Weiland and has been continually developed over the years [25]. This method covers the full frequency range of electromagnetics (from static up to high frequency) and optical applications and is the basis not only for the CST transient solver but also for other commercial simulation tools [26].

III. Antenna models

The simulations included a model of a GPR antenna that is representative of a Geophysical Survey Systems, Inc. (GSSI) 1.5 GHz (centre frequency) antenna, and a model of a GPR antenna that is representative of a MALÅ GeoScience (MALÅ) 1.2 GHz (centre frequency) antenna. The antenna models include all of the main features and geometry of the real antennas. Details of the development of antenna models and initial validation can be found in [13]. Fig. 1 and Fig. 2 show photographs of the real antennas and views of the detailed geometry of the antenna models from gprMax and CST. A spatial discretisation of $\Delta x = \Delta y = \Delta z = 1$ mm was chosen as a good compromise between accuracy and computational resources. The Courant Friedrichs Lewy (CFL) condition was enforced which resulted in a time-step of Δt = 1.926 ps.

IV. Experimental and simulated antenna responses

Experimental and simulated responses were taken in the following four environments:

1) Free space (crosstalk) response of GSSI 1.5 GHz antenna and MALÅ 1.2 GHz antenna
2) Response of of GSSI 1.5 GHz antenna in a lossy dielectric environment of permittivity, $\epsilon_r = 32$, and complex conductivity
3) Response of of GSSI 1.5 GHz antenna in a lossy dielectric environment of permittivity, $\epsilon_r = 10$, and complex conductivity with a 12 mm steel rebar target
4) Response of of GSSI 1.5 GHz antenna in a lossy dielectric environment of permittivity, $\epsilon_r = 32$, and complex conductivity with a 12 mm steel rebar target

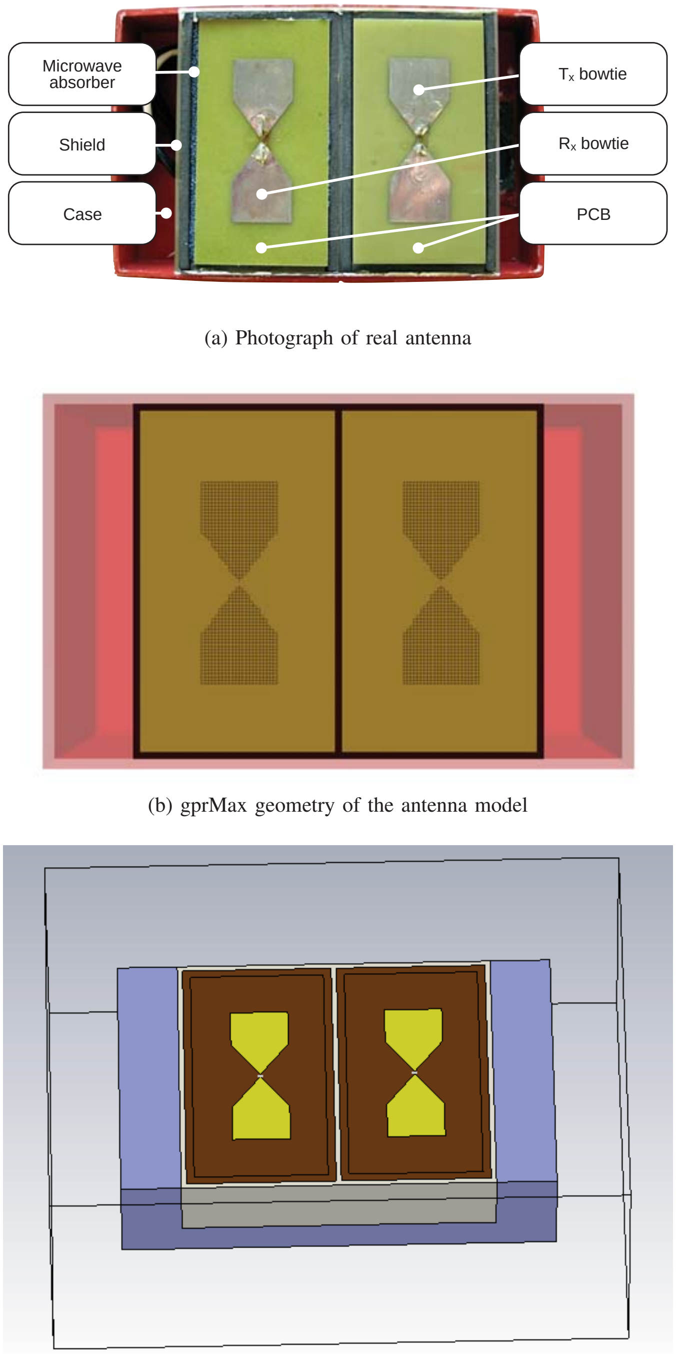

(a) Photograph of real antenna

(b) gprMax geometry of the antenna model

(c) CST geometry of the antenna model

Fig. 1. GSSI 1.5 GHz antenna

A series of oil-in-water (O/W) emulsions were used to simulate lossy dielectric environments. The permittivity and conductivity of the emulsions were set by controlling ratios of the constituent chemicals [13]. A further advantage of using liquids was the ease with which targets could be positioned. The main components of the experimental apparatus were: a 50 litre galvanised steel tank (610 mm × 400 mm × 210 mm); a plastic rig to mount and position the antenna and the 12 mm

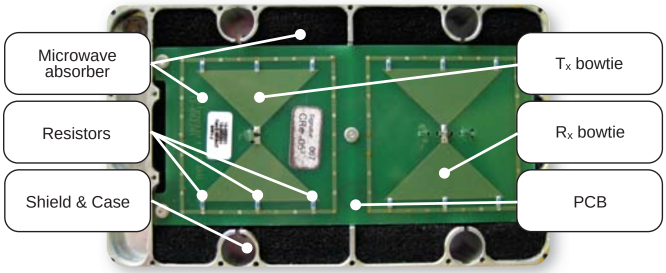

(a) Photograph of real antenna

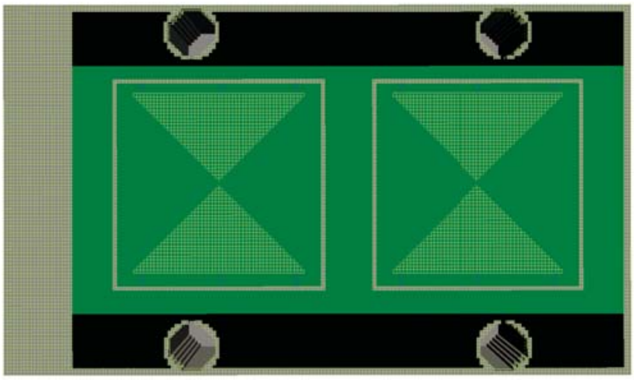

(b) gprMax geometry of the antenna model

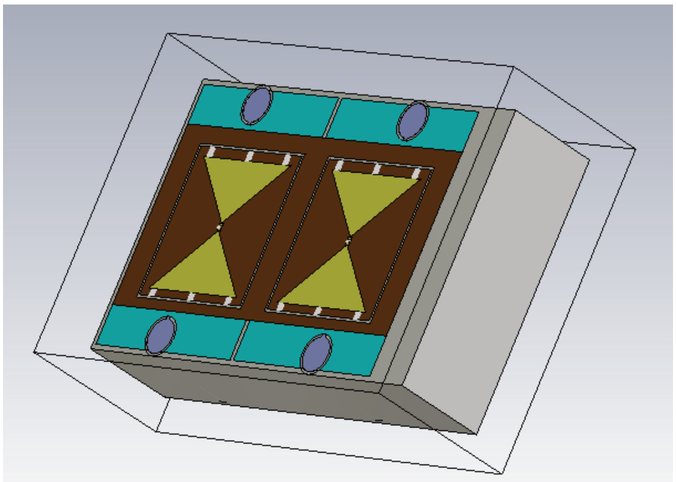

(c) CST geometry of the antenna model

Fig. 2. MALÅ 1.2 GHz antenna

steel rebar target; and the GPR system and antenna.

Fig. 3 and Fig. 4 present the responses of the antennas in free space. There is very good agreement between the phase and amplitude of the simulated responses. It was found that to obtain a good match between the two simulations the resistance at the feed point of the antenna was different. The feeding model being used in the CST simulation is not known. Therefore the difference in source resistances could well be attributed to the use of different feed models.

Fig. 5 presents the responses of the antennas over a lossy

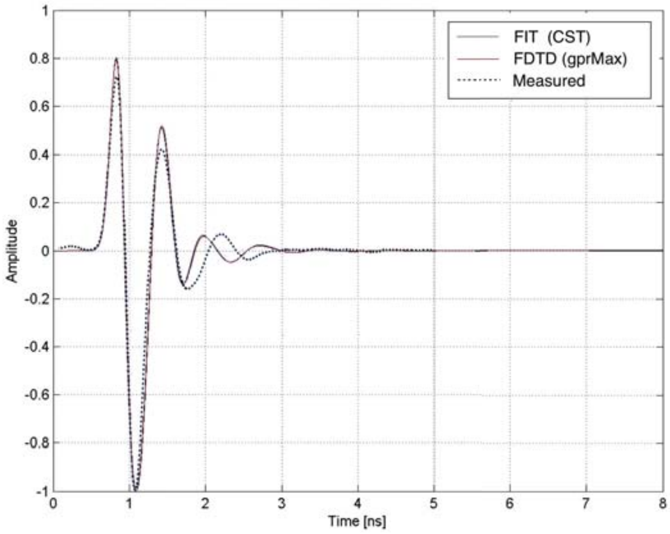

Fig. 3. Experimental and simulated responses from a GSSI 1.5 GHz antenna in free space.

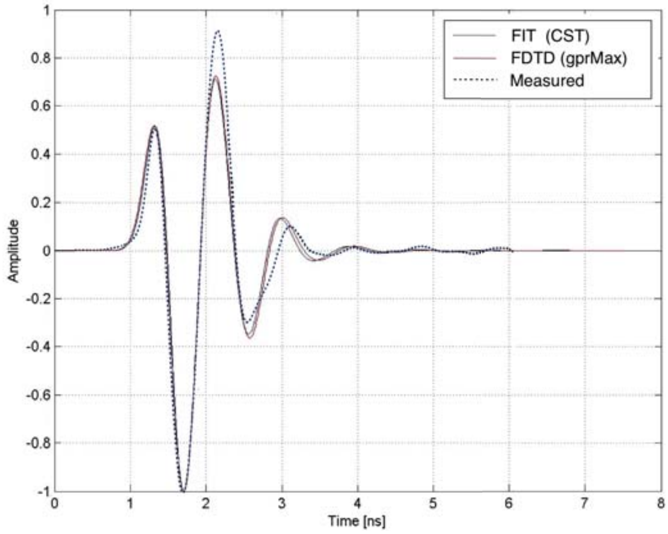

Fig. 4. Experimental and simulated responses from a MALÅ 1.2 GHz antenna in free space.

dielectric environment of permittivity, $\epsilon_r = 32$. The direct wave (propagation from transmitter to receiver) and a reflected wave (from the bottom of the steel tank) are evident. There is good agreement between the phase and amplitude of the experimental and simulated responses. However, the differences demonstrate that even in such a simple environment the electromagnetic wave propagation is still complex. The emulsion is a lossy dielectric with a complex, frequency-dependent conductivity. Both simulations used a Debye model with an additional constant DC conductivity term to replicate this dispersive behaviour. The Debye formulation is given by (1) and the parameters used are given in Table I.

$$\chi(t) = \frac{\Delta\epsilon_r}{\tau} e^{-t/\tau}, \qquad (1)$$

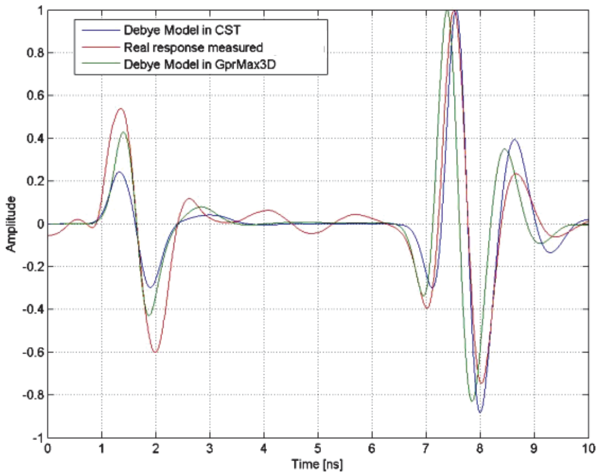

Fig. 5. Experimental and simulated responses from a GSSI 1.5 GHz antenna in a lossy dielectric environment of permittivity, $\epsilon_r = 32$, and complex conductivity.

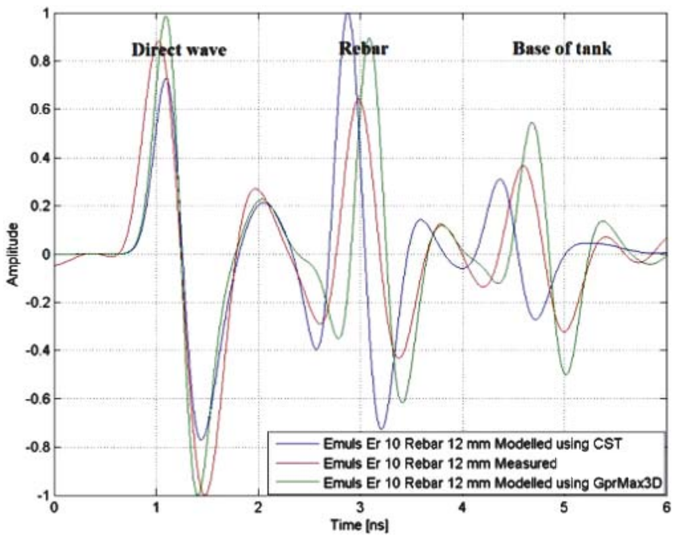

Fig. 6. Experimental and simulated responses from a GSSI 1.5 GHz antenna in a lossy dielectric environment of permittivity, $\epsilon_r = 10$, and complex conductivity with a 12 mm steel rebar target.

where $\Delta\epsilon_r = \epsilon_{rs} - \epsilon_{r\infty}$, ϵ_{rs} is the zero-frequency relative permittivity, $\epsilon_{r\infty}$ is the relative permittivity at infinite frequency, and τ is the pole relaxation time.

Fig. 6 and Fig. 7 present the responses of the antennas to a 12 mm diameter steel rebar embedded in lossy dielectric environments of permittivity, $\epsilon_r = 10$ and $\epsilon_r = 32$. There are now three overlapping parts to the response, the direct wave,

	ϵ_{rs}	$\epsilon_{r\infty}$	τ (ps)
Emulsion 1	10.34	4.0	9.95
Emulsion 2	32.03	1.0	7.50

TABLE I
DEBYE EQUATION PARAMETERS FOR MODELLING THE COMPLEX CONDUCTIVITY OF THE EMULSIONS

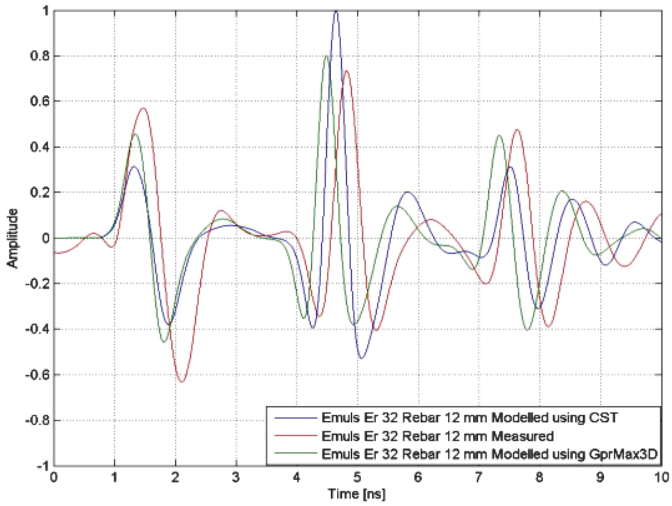

Fig. 7. Experimental and simulated responses from a GSSI 1.5 GHz antenna in a lossy dielectric environment of permittivity, $\epsilon_r = 32$, and complex conductivity with a 12 mm steel rebar target.

the reflected wave from the rebar, and the reflected wave from the bottom of the steel tank. Again, the fundamental amplitude and phase information from the simulated data agrees with the experimental measurements.

V. Conclusion

Models of two commercial high-frequency GPR antennas have been developed and used with two commonly used simulation tools. The models include all the main features and geometry of the real antennas. The models were used to compare free space responses and responses in lossy dielectric environments with experimental data. Good agreement between the phase and amplitude of the experimental data and the two simulations is evident. This cannot be attained by only using a simple infinitesimal dipole model in a simulation – a realistic model of the antenna is required. Differences that were evident between the simulated data, highlight the importance of understanding how features such as material dispersion and antenna feeding are modelled in simulations. This is particularly relevant for the many GPR applications which operate in the near-field of the antenna, where the interaction between the antenna, the ground/structure and targets is important.

Acknowledgment

This work benefited from networking activities carried out within the EU funded COST Action TU1208 "Civil Engineering Applications of Ground Penetrating Radar."

References

[1] L. Gurel and U. Oguz, "Three-dimensional fdtd modeling of a ground-penetrating radar," *Geoscience and Remote Sensing, IEEE Transactions on*, vol. 38, no. 4, pp. 1513–1521, 2000.

[2] G. Klysz, X. Ferrieres, J. Balayssac, and S. Laurens, "Simulation of direct wave propagation by numerical fdtd for a gpr coupled antenna," *NDT & E International*, vol. 39, no. 4, pp. 338–347, 2006.

[3] S. Lambot, E. C. Slob, I. van den Bosch, B. Stockbroeckx, and M. Vanclooster, “Modeling of ground-penetrating radar for accurate characterization of subsurface electric properties,” *Geoscience and Remote Sensing, IEEE Transactions on*, vol. 42, no. 11, pp. 2555–2568, 2004.

[4] B. Lampe and K. Holliger, “Numerical modeling of a complete ground-penetrating radar system,” in *International Symposium on Optical Science and Technology*. International Society for Optics and Photonics, 2001, pp. 99–110.

[5] K.-H. Lee, C.-C. Chen, F. L. Teixeira, and K.-H. Lee, “Modeling and investigation of a geometrically complex uwb gpr antenna using fdtd,” *Antennas and Propagation, IEEE Transactions on*, vol. 52, no. 8, pp. 1983–1991, 2004.

[6] Y. Nishioka, O. Maeshima, T. Uno, and S. Adachi, “Fdtd analysis of resistor-loaded bow-tie antennas covered with ferrite-coated conducting cavity for subsurface radar,” *Antennas and Propagation, IEEE Transactions on*, vol. 47, no. 6, pp. 970–977, 1999.

[7] V. Pérez-Gracia, D. Di Capua, R. González-Drigo, and L. Pujades, “Laboratory characterization of a gpr antenna for high-resolution testing: Radiation pattern and vertical resolution,” *NDT & E International*, vol. 42, no. 4, pp. 336–344, 2009.

[8] R. L. Roberts and J. J. Daniels, “Modeling near-field gpr in three dimensions using the fdtd method,” *Geophysics*, vol. 62, no. 4, pp. 1114–1126, 1997.

[9] F. L. Teixeira, W. C. Chew, M. Straka, M. Oristaglio, and T. Wang, “Finite-difference time-domain simulation of ground penetrating radar on dispersive, inhomogeneous, and conductive soils,” *Geoscience and Remote Sensing, IEEE Transactions on*, vol. 36, no. 6, pp. 1928–1937, 1998.

[10] D. Uduwawala, M. Norgren, P. Fuks, and A. W. Gunawardena, “A deep parametric study of resistor-loaded bow-tie antennas for ground-penetrating radar applications using fdtd,” *Geoscience and Remote Sensing, IEEE Transactions on*, vol. 42, no. 4, pp. 732–742, 2004.

[11] N. Diamanti and A. P. Annan, “Characterizing the energy distribution around gpr antennas,” *Journal of Applied Geophysics*, vol. 99, pp. 83–90, 2013.

[12] N. Diamanti, P. Annan, and D. Redman, “Quantifying gpr transient waveforms in the intermediate zone,” in *Advanced Ground Penetrating Radar (IWAGPR), 2013 7th International Workshop on*. IEEE, 2013, pp. 1–7.

[13] C. Warren and A. Giannopoulos, “Creating FDTD models of commercial GPR antennas using Taguchi’s optimisation method,” *Geophysics*, vol. 76, no. 2, pp. G37–G47, 2011.

[14] K. S. Yee, “Numerical solution of initial boundary value problems involving maxwells equations in isotropic media,” *Antennas and Propagation, IEEE Transactions on*, vol. 14, no. 3, pp. 302–307, 1966.

[15] A. Giannopoulos, “Modelling ground penetrating radar by gprmax,” *Construction and building materials*, vol. 19, no. 10, pp. 755–762, 2005.

[16] N. J. Cassidy and T. M. Millington, “The application of finite-difference time-domain modelling for the assessment of gpr in magnetically lossy materials,” *Journal of Applied Geophysics*, vol. 67, no. 4, pp. 296–308, 2009.

[17] P. Shangguan and I. L. Al-Qadi, “Calibration of fdtd simulation of gpr signal for asphalt pavement compaction monitoring,” *Geoscience and Remote Sensing, IEEE Transactions on*, vol. 53, no. 3, pp. 1538–1548, 2015.

[18] E. Slob, M. Sato, and G. Olhoeft, “Surface and borehole ground-penetrating-radar developments,” *Geophysics*, vol. 75, no. 5, pp. 75A103–75A120, 2010.

[19] F. Soldovieri, J. Hugenschmidt, R. Persico, and G. Leone, “A linear inverse scattering algorithm for realistic GPR applications,” *Near Surface Geophysics*, vol. 5, no. 1, pp. 29–42, 2007.

[20] M. Solla, H. Lorenzo, F. Rial, and A. Novo, “Ground-penetrating radar for the structural evaluation of masonry bridges: Results and interpretational tools,” *Construction and Building Materials*, vol. 29, pp. 458–465, 2012.

[21] A. P. Tran, F. Andre, and S. Lambot, “Validation of near-field ground-penetrating radar modeling using full-wave inversion for soil moisture estimation,” *Geoscience and Remote Sensing, IEEE Transactions on*, vol. 52, no. 9, pp. 5483–5497, 2014.

[22] Elsevier. Scopus, the largest abstract and citation database of peer-reviewed literature. [Online]. Available: http://www.scopus.com

[23] Python Software Foundation. Python. [Online]. Available: https://www.python.org/

[24] C. Warren, A. Giannopoulos, and I. Giannakis, “An advanced gpr modelling framework: The next generation of gprmax,” in *Advanced Ground Penetrating Radar (IWAGPR), 2015 8th International Workshop on*. IEEE, 2015, pp. 1–4.

[25] T. Weiland, “A discretization model for the solution of maxwell’s equations for six-component fields,” *Archiv Elektronik und Uebertragungstechnik*, vol. 31, pp. 116–120, 1977.

[26] Mentor Graphics. Electromagnetic simulation solutions. [Online]. Available: https://www.mentor.com/pcb/nimbic/